Gap reduction vs. geometric deviation: a trade-off in composite assembly

Citation for the original published paper (version of record):

Toyoda, D., Sadeghi Tabar, R., Lindkvist, L. et al (2026). Gap reduction vs. geometric deviation: a trade-off in composite assembly. Procedia CIRP, 145: 37-42.
http://dx.doi.org/10.1016/j.procir.2026.03.134

Available online at www.sciencedirect.com

ScienceDirect

Procedia CIRP 145 (2026) 37–42

www.elsevier.com/locate/procedia

19th CIRP Conference on Computer-Aided Tolerancing (CAT 2026)

Gap reduction vs. geometric deviation: a trade-off in composite assembly

Diogo Toyoda[a,*], Roham Sadeghi Tabar[a], Lars Lindkvist[a], Kristina Wärmefjord[a], Rikard Söderberg[a]

[a]*Department of Industrial and Materials Science, Chalmers University of Technology, SE-41296, Gothenburg, Sweden*

* Corresponding author. Tel.: +46-72-397-2193. *E-mail address:* toyoda@chalmers.se

Abstract

In the assembly of large-scale composite structures, interface gaps arising from part deviations are commonly filled with shims to avoid induced stresses due to the forced contact. However, excessive shim thickness increases bending stresses in fasteners, while the process of gap minimization itself can distort the final assembly shape. This study presents a framework that integrates fastener load limits with fixture optimization to determine maximum allowable shim thickness and reduce interface gaps. Using a combination of finite element simulation, contact modeling, and numerical optimization, the method computes optimal fixture adjustments to minimize gaps while respecting structural constraints. A case study on a simplified wingbox section shows that, although local gaps are reduced by an average of 43%, global geometric deviations often increase, revealing a fundamental trade-off between gap minimization and geometric accuracy. The framework supports pre-manufactured shims and is particularly suited for digital-twin environments, enabling inspection data to inform fixture setup before assembly. Results highlight the importance of jointly considering structural and geometric objectives and suggest that multi-objective optimization and alternative shimming strategies can further enhance geometry assurance and joint integrity.

Keywords: shimming; fixture adjustment; composites; geometry assurance; digital twin

1. Introduction

In the assembly of large-scale composite structures, such as aerospace components, unavoidable part and process geometric deviations often lead to gaps between parts. These gaps pose a particular challenge for composite materials. If fasteners, like rivets, pins/collars or bolts are installed while these gaps are present, the resulting forced contact can introduce unintended stresses and additional part distortions, that can directly cause structural damage, such as delamination and matrix cracking [1].

Shims are commonly used to fill these gaps, but introduce their own challenges. By modifying the load path, shims can increase bending stresses in the fasteners and affect the structural response of the assembly [2]. Despite their widespread use, current geometry assurance workflows lack an integrated framework that links fixture adjustment directly to the structural load limits of the fasteners. This work addresses this gap by proposing a framework where fastener load limits serve as the primary constraint for fixture optimization, allowing for an explicit evaluation of the trade-off between structural joint integrity and global dimensional accuracy. In this work, shimming refers exclusively to the filling of interface gaps with solid or liquid materials. It does not include locator adjustment, although shimming and trimming are sometimes used with that meaning.

This paper presents a framework that determines the maximum allowable shim thickness based on part thickness and fastener strength, and computes fixture adjustments that reduce gaps while respecting these structural limits. While the optimization prioritizes joint integrity, we perform a post-process analysis on the resulting assembled geometry. This work demonstrates that minimizing local interface gaps to satisfy structural constraints can lead to increased global geometric deviations in compliant composite assemblies. This highlights the inherent trade-off that must be managed in geometry assurance workflows.

2. Theoretical framework and methodology

This section presents the theoretical background and methodological choices underlying the proposed framework.

2212-8271 © 2026 The Authors. Published by Elsevier B.V.

10.1016/j.procir.2026.03.134

2.1. Shim limits calculation

To minimize the adverse mechanical effects that shims introduce into a joint, the shim thickness should be kept as small as possible. Rules of thumb can be found in the literature for defining acceptable shim thickness limits [3]. This section outlines the procedure adopted in this study to determine the maximum allowable shim thickness. A schematic of a single-shear joint and the corresponding shear load acting on the fastener is shown in Fig. 1.

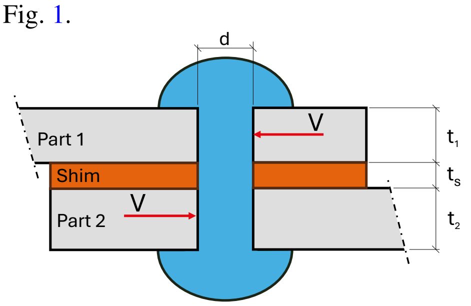

Fig. 1. Single-shear shimmed joint representation with shear load acting on fastener

From classical beam theory [4], the bending and shear stresses in the fastener in an unshimmed joint (Eq. 1) are respectively:

$$\sigma_b^0 = \frac{32V}{\pi d^3} e_0, \qquad \tau = \frac{4V}{\pi d^2}, \qquad \text{where } e_0 = \frac{t_1 + t_2}{2}, \tag{1}$$

V is the shear load, d is the fastener diameter, e_0 is the bending arm in an idealized condition where the fastener is loaded in shear at the mid-plane of each part and t_1 and t_2 are the thicknesses of the parts.

The Von Mises equivalent stress and the increased bending stress in the fastener caused by the shim can be expressed as Eq. 2:

$$\sigma_{eq} = \sqrt{\sigma_b^2 + 3\tau^2}, \qquad \sigma_b = \sigma_b^0 \left(1 + \frac{t_s}{2e_0}\right), \tag{2}$$

where t_s is the shim thickness.

The factor $k = 1 + f$ is introduced, where f is the maximum allowed additional Von Mises stress. By combining Eqs. 1 and 2 and solving for t_s, the maximum shim thickness is derived as:

$$t_s^{max} = 2e_0 \left(\sqrt{k^2 + (k^2 - 1)\frac{3}{64}\frac{d^2}{e_0^2}} - 1 \right) \tag{3}$$

Calculated values of t_s^{max} will be used as boundaries in the optimization problem.

2.2. Assembly simulation and gaps prediction

In industrial practice, the assembly process for compliant structures begins with positioning each component in an assembly fixture. Due to inherent part and process-induced deviations, this positioning often results in contact forces and gaps. These gaps are measured with feeler gauges to determine shim thicknesses, which are manufactured while the assembly is disassembled for shim installation before final fastening [5].

Numerically, part deviations are simulated in this work by introducing imposed nodal displacements, with the resulting deformed shapes generated using the finite element method (FEM). These displacements are scaled to typical manufacturing tolerances, representing characteristic deviations such as those derived from the curing process. Surface roughness is excluded from the model as its typical magnitude is negligible compared to overall geometric deviations. Furthermore, as the focus remains on the macro-mechanical gap reduction, friction is not considered in this study. Each deviated part is then positioned in a virtual assembly fixture. Contact modeling is employed to prevent part penetration and compute contact forces. The method of influence coefficients (MIC), coupled with FEM, is then used to efficiently evaluate the resulting assembly configuration and gap distributions [6].

Several studies have investigated gap prediction using different approaches, such as measurement-driven numerical procedures [7, 8], mode shape decomposition model for statistical analysis [9] and physics-based multi-stage simulation [10]. In [11], a single-step shimming strategy is proposed, automatically choosing between solid or liquid shim, while FEM and in-line measurements are used in [5, 12] to predict shim geometry. The strategy proposed in this paper extends these works by explicitly integrating allowable shim thickness limits derived from joint mechanics into the gap reduction process.

2.3. Assembly locators adjustment

A rigid part has six degrees of freedom (three translations and three rotations), which must be constrained by the fixture, typically using the classic 3-2-1 locating scheme. For compliant parts, such as the thin composite structures considered in this work, additional support points are required to counteract external loads and ensure proper positioning.

Locator adjustment is a geometry assurance technique used in assemblies to improve the dimensional quality of the final product by making small, controlled modifications to the positions of the locators in an assembly fixture, as demonstrated in [13, 14].

In this study, locator adjustment is implemented as an optimization process. The objective is to determine the optimal adjustment for each locator, specifically in its constraining direction, to minimize initial gaps between parts. The locators position and constraining directions of the case study are shown in Fig. 2 by the red (main locating system) and orange arrows (support points). This optimization of the fixture configuration to accommodate part variations serves as a first step for reducing shim requirements, thereby minimizing the adverse mechanical effects that shims introduce in structural joints.

2.3.1. Optimization

The optimization problem was formulated as the locator adjustment problem in [15], and modified to reflect the maximum allowable limit on the shims:

$$\begin{aligned} \min_{u} \quad & \tau_{\mu}(u) \\ \text{s.t.} \quad & \alpha \leq u_i \leq \beta, \quad i = 1, \dots, z \\ & t_s(u) \leq t_s^{\max} \end{aligned} \tag{4}$$

Here, $\tau_{\mu}(u)$ is the root mean square (RMS) of all the gaps between parts at fastener positions, u is a vector of scalar adjustments applied to the positions of the z clamps, $u = [u_1, \dots, u_z]$. The bounds α and β are the maximum allowable adjustments for each fixture point. These limits are set to ±2 mm, based on common industrial shimming practice.

The constraint $t_s(u) \leq t_s^{max}$ ensures that the optimization reduces gaps while respecting the maximum allowable shim thickness and limiting additional Von Mises stress, $f_{\max}$, set to 15% to maintain sufficient margin for in-service loads.

The problem is framed as a constrained black-box optimization. To reduce the number of function evaluations through the computer-aided tolerancing (CAT) software, a trust-region reflective approach [16] is employed. Here, a locally linear surrogate of the gap field is obtained through a finite difference method. With a two-step approach, the constraints are taken into account initially by solving an unconstrained penalty problem for the allowable adjustments and secondly by a quadratic surrogate formulation with the maximum shim thickness. The approach is implemented in Python, and for each part in the assembly and for each locator, the software is called twice to evaluate the gaps.

2.4. Shimming simulation and geometric output

After the gaps are minimized, shimming is simulated by modifying the nominal separation between the parts according to the predicted gap distribution. In this step, the entire gap is assumed to be filled, either with a liquid shim or a combination of solid and liquid materials. Next, fastener installation is simulated using rigid beam elements, which constrain all six degrees of freedom of the connected nodes. The assembled structure is then released from the assembly fixture and positioned in a virtual inspection fixture. In this unloaded state, after the relaxation of fixture-induced stresses, the resulting geometric deviations are evaluated relative to the nominal geometry.

The assembly process is simulated using the CAT software RD&T, which integrates an internal FEM solver, contact and fastener modeling, and the method of influence coefficients (MIC) to simulate the complete assembly process [17].

The proposed framework can be summarized as follows:

1. The maximum allowable shim thickness is computed for each interface using Eq. 3;
2. Part deviations are simulated and each part is positioned in a virtual fixture, with gaps evaluated via MIC, FEM and contact modeling;
3. The fixture optimization (Eq. 4) adjusts locator positions to minimize gaps while respecting the shim thickness constraints;
4. Shimming and fastening are simulated on the optimized configuration, again via MIC, FEM and contact modeling, and the resulting geometric deviations are evaluated after fixture release.

Following this procedure, the framework is applied to a case study of a simplified wingbox section assembly, described in the next section.

3. Case study

The case study is a simplified wingbox section assembly, comprised of five parts: upper and lower skins, front and rear spars and rib, as seen in Fig. 2. All parts are made of carbon fiber reinforced polymer (CFRP) bidirectional fabric impregnated with epoxy resin. Ten different deviated parts are generated for each part, as described in Sec. 2.2, resulting in ten assemblies.

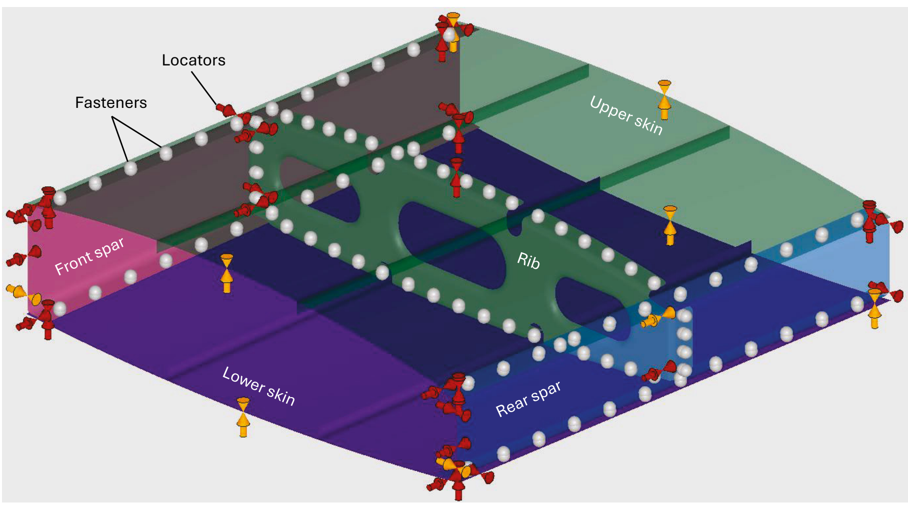

Fig. 2. Assembly with positioning system (arrows) and fasteners (spheres)

The fiber and resin properties are based on [18]. The rule-of-mixture formulation with iso-strain assumptions (Voigt model) was employed to calculate the fabric properties, which are listed in Table 1. E denotes the elastic modulus, G is the shear modulus and ν is the Poisson's ratio. The subscript 1 refers to the longitudinal, 2 to the transverse and 3 to the out-of-plane direction. Each layer is 0.5 mm thick and classical laminate theory is used to calculate the laminate properties. The composite anisotropic behavior is taken into account by the FEM model, using shell elements in the midplane.

Table 1. Layer properties (iso-strain assumptions)

Property	Value	Unit
E_1, E_2	51.3	GPa
E_3	15.9	GPa
G_{12}	14.5	GPa
G_{13}, G_{23}	18.2	GPa
ν_{12}	0.024	-
ν_{13}, ν_{23}	0.155	-

The total thickness and layup of each part are detailed in Table 2. The assembly is joined by 89 fasteners distributed across the eight interfaces detailed in Table 3 and 1222 contact points were identified. The fastener diameter and maximum allowed shim thickness of each interface, according to Eq. 3, are also shown in Table 3.

Table 2. Parts' thickness and layup

Part	Thickness [mm]	Layup [deg]
Rib	1.5	[0/90, ±45, 0/90]
Lower Skin	1.5	[0/90, ±45, 0/90]
Upper Skin	1.0	[0/90, 0/90]
Front Spar	2.0	$[0/90, \pm45]_s$
Rear Spar	3.0	$[0/90, \pm45, 0/90]_s$

Table 3. Fasteners diameter and maximum shim thickness for each interface

Part 1	Part 2	d [mm]	t_s^{max} [mm]
Upper skin	Rear spar	4.0	0.70
Lower skin	Rear spar	5.0	0.82
Upper skin	Front spar	4.0	0.59
Lower skin	Front spar	4.0	0.64
Front spar	Rib	4.0	0.64
Rear spar	Rib	5.0	0.82
Lower skin	Rib	4.0	0.59
Upper skin	Rib	4.0	0.54

4. Results and discussion

After running the optimization algorithm, the locators were adjusted, resulting in reduced gaps between parts. Fig. 3 shows the RMS gaps for the nominal and adjusted fixtures. Across all ten assemblies, the average RMS gaps decreased from 0.185 to 0.103 mm, representing an average reduction of 43%. The maximum average gap was similarly reduced, from 0.62 to 0.35 mm.

Therefore, the algorithm successfully reduced assembly interface gaps, staying within the maximum allowed adjustment

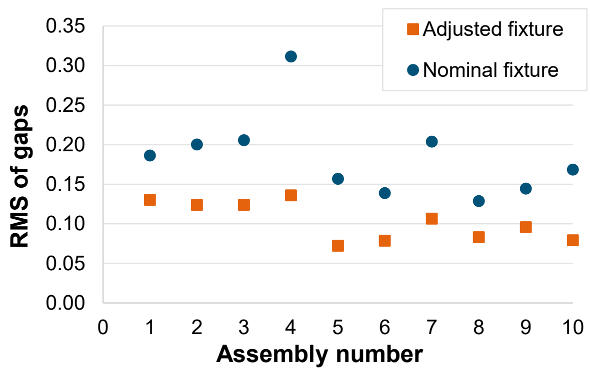

Fig. 3. RMS gaps with nominal and adjusted fixture

of 2 mm. In all ten cases, the largest adjustment was 0.86 mm, highlighting that significant improvements in gap reduction can be achieved through relatively small fixture adjustments.

The gap distribution is illustrated in Fig. 4, while the corresponding geometric deviations after release from the assembly fixture are shown in Fig. 5. Although different patterns were observed across the ten assemblies, only assembly 1, with the highest fixture adjustment and geometric deviations RMS, is shown for illustration.

Regarding geometric deviations, the average RMS nodal displacements after release from the assembly fixture can be compared between the shimmed assembly in the nominal fixture and the assembly in the adjusted fixture. The average RMS displacement increased from 0.641 mm in the nominal fixture to 1.004 mm in the adjusted fixture. Despite the reduction in local gaps, the resulting geometry of the shimmed assembly was degraded in most cases (7 out of 10), as shown in Table 4.

However, using the nominal fixture would require shims thicker than the allowable limit, which would introduce a more significant structural penalty on the fasteners ($f > 20\%$). This demonstrates that gap minimization and geometric accuracy are not directly aligned objectives in compliant assemblies.

Table 4. Average RMS displacement, in mm, in nominal and adjusted fixture

Assembly	Nominal fixture	Adjusted fixture	Difference
1	0.82	1.91	-1.09
2	0.88	1.59	-0.72
3	0.43	0.34	0.08
4	0.87	0.95	-0.09
5	0.97	1.08	-0.11
6	0.62	1.50	-0.88
7	0.68	0.54	0.14
8	0.32	0.42	-0.10
9	0.35	1.34	-0.99
10	0.47	0.36	0.11

Analyzing the results, a strong correlation was observed between the RMS magnitude of fixture-point adjustments and the RMS Tsai-Hill criteria values [19] in the assembly fixture ($r = 0.75$). Similarly, a significant correlation ($r = 0.73$) was found between the RMS Tsai-Hill criteria and the RMS geo-

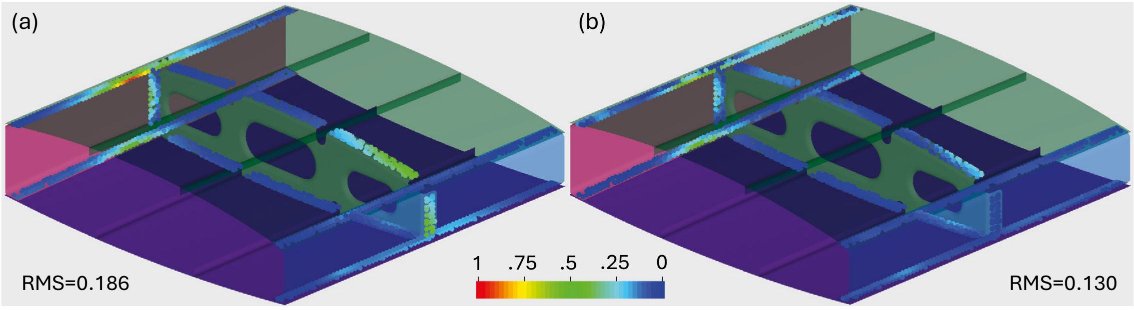

Fig. 4. Gap distribution in assembly 1 with (a) nominal fixture and (b) adjusted fixture

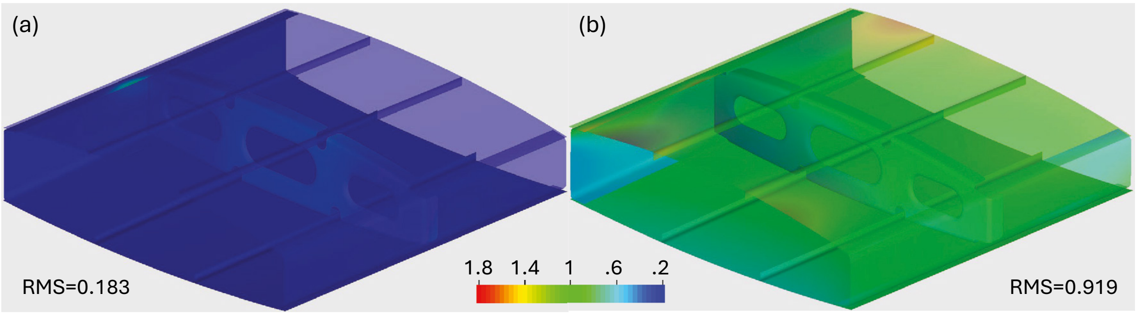

Fig. 5. Geometric deviations in shimmed assembly 1 with (a) nominal fixture and (b) adjusted fixture

metric deviations (nodal displacements). These correlations are illustrated in Fig. 6.

Minimizing gaps often introduces forced contact conditions, which locally increase bending and stresses. Upon fixture release, these stresses relax, potentially producing larger global deviations even when assembly gaps have been reduced. Furthermore, fixture adjustments displace the assembly from its nominal geometry, further contributing to the observed deviations. The resulting shimmed assembly geometry, however, is likely influenced by several interdependent factors, including: (1) part deviations relative to regions with larger gaps; (2) part deviations relative to locator positions; (3) locator positions relative to regions with larger gaps; (4) direction of locator adjustments relative to nearby gap directions; and (5) local part stiffness.

5. Conclusion

This study examined the trade-offs between gap minimization, shim thickness constraints, and geometric accuracy in the assembly of compliant composite structures. A methodology was developed to determine maximum allowable shim thickness based on fastener shear load capacity and integrated into a fixture-optimization framework. While the approach effectively reduced shim requirements, it often led to degraded global geometric accuracy. This reveals a fundamental conflict between

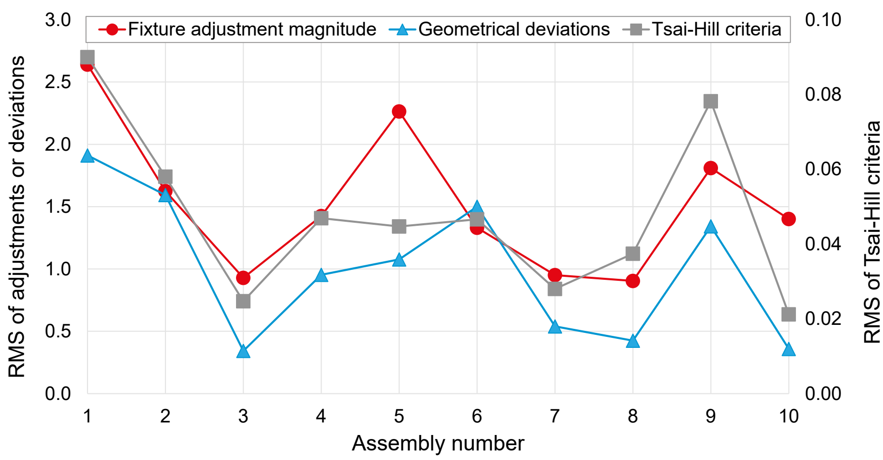

Fig. 6. Correlations between fixture adjustment magnitude, geometric deviations and stress (Tsai-Hill)

two key assembly objectives: reducing local gaps and preserving the final geometry. The nominal fixture maintains geometric fidelity but requires shims beyond allowable limits, increasing fastener loads, whereas the adjusted fixture yields structurally acceptable shim levels but tends to distort the assembled shape.

The proposed framework enables shims to be defined and manufactured before the parts enter the fixture, eliminating pre-assembly steps. This capability is particularly valuable in a digital-twin environment, where inspection data can flow directly into the assembly model and fixture settings can be prepared in advance. Since large assemblies such as wingboxes already rely on individual inspections of major components, the method introduces no additional measurement burden and can also support selective assembly strategies.

The optimization may fail to find feasible solutions when geometric deviations are large or when both gap and structural constraints are tight. Early identification of such cases is beneficial, allowing design modifications or relaxed limits to be considered before production. Potential mitigation strategies include adjusting fixture ranges, prioritizing specific fastener locations, or introducing weighted objectives to balance geometric and structural criteria. More advanced adaptive or multi-objective algorithms could further improve feasibility and performance.

Future research should incorporate discrete shim thicknesses, such as peelable solid shims, and explore alternative constraint formulations based on allowable assembly stresses rather than shim thickness alone. Fastening with controlled gaps could then be permitted when stresses remain below material limits and sufficient margin is retained for operational loads. A comprehensive multi-objective optimization, simultaneously addressing joint strength, geometric accuracy, and stress levels, together with a more detailed representation of shimming and part-deviation propagation, would enhance the predictive capability and robustness of digital-twin-based assembly planning.

Acknowledgements

This work was carried out at Wingquist Laboratory and the Area of Advance Production at Chalmers within the project “Resilient manufacturing of composites (RECO)”, financed by the strategic innovation program Produktion2030, supported by Vinnova. The support is gratefully acknowledged.

Declaration of generative AI and AI-assisted technologies in the manuscript preparation process

During the preparation of this work the authors used ChatGPT in order to assist with language editing and clarity. After using this tool/service, the authors reviewed and edited the content as needed and take full responsibility for the content of the published article.

References

[1] Comer, A., Dhôte, J., Stanley, W., Young, T.. Thermo-mechanical fatigue analysis of liquid shim in mechanically fastened hybrid joints for aerospace applications. Compos Struct 2012;94(7):2181–2187. doi:https://doi.org/10.1016/j.compstruct.2012.01.008.

[2] Cheng, L., Wang, Q., Ke, Y.. Experimental and numerical analyses of the shimming effect on bolted joints with nonuniform gaps. Proc Inst Mech Eng, Part C: J Mech Eng Sci 2019;233(11):3964–3975. doi:https://doi.org/10.1177/0954406218809139.

[3] Niu, M.C.Y.. Airframe Stress Analysis and Sizing. 2nd ed.; Hong Kong/USA: Adastra Engineering Center; 1999.

[4] Öchsner, A.. Classical beam theories of structural mechanics; vol. 42. Springer; 2021.

[5] Franciosa, P., Gerbino, S., Stella, E., Berri, L., Gramegna, N., Gallo, N., et al. A digital twin approach for smart assembly of aircraft skin panels with mechanical fasteners. In: Int. Jt. Conf. Mech. Des. Eng. Adv. Manuf. Springer; 2022, p. 851–861. doi:https://doi.org/10.1007/978-3-031-15928-2_74.

[6] Dahlström, S., Lindkvist, L.. Variation simulation of sheet metal assemblies using the method of influence coefficients with contact modeling. J Manuf Sci Eng 2007;129:615–622. doi:https://doi.org/10.1115/1.2714570.

[7] Lacroix, C., Mathieu, L., Thiébaut, F., Douilly, M., Falgarone, H.. Numerical process based on measuring data for gap prediction of an assembly. Procedia CIRP 2015;27:97–102. doi:https://doi.org/10.1016/j.procir.2015.04.050.

[8] Yang, Y., Jin, Y., Price, M., Abdelal, G., Maropoulos, P., Higgins, C.. Gap volume prediction for aircraft wing assembly. Procedia Manuf 2021;54:227–232. doi:https://doi.org/10.1016/j.promfg.2021.07.035.

[9] Zaitseva, N., Lupuleac, S., Shinder, J.. Initial gap modeling for wing assembly analysis. Aerosp Syst 2025;8(1):163–169. doi:https://doi.org/10.1007/s42401-024-00302-4.

[10] Esposito, C., Cosenza, C., Gerbino, S., Martorelli, M., Franciosa, P.. Virtual shimming simulation for smart assembly of aircraft skin panels based on a physics-driven digital twin. Int J Interact Des Manuf 2022;16(2):753–763. doi:https://doi.org/10.1007/s12008-022-00875-4.

[11] Ehmke, F., Rao, S., Wollnack, J.. Single step shimming solution for automated aircraft assembly. In: IEEE Conf. Autom. Sci. Eng. IEEE; 2017, p. 662–667. doi:https://doi.org/10.1109/COASE.2017.8256179.

[12] Ospina-Aldana, G., Hassan Ali, M.I., Odendaal, H., Abusafieh, A.A., Woon, W.. Predictive shimming of frame-panel assemblies using fem and laser scanning. In: ASME Int. Mech. Eng. Congr. Expo.; vol. 59377. American Society of Mechanical Engineers; 2019, p. V02AT02A047. doi:https://doi.org/10.1115/IMECE2019-11232.

[13] Forslund, A., Lorin, S., Lindkvist, L., Wärmefjord, K., Söderberg, R.. Minimizing weld variation effects using permutation genetic algorithms and virtual locator trimming. J Comput Inf Sci Eng 2018;18(4):041010. doi:https://doi.org/10.1115/1.4040952.

[14] Rezaei Aderiani, A., Wärmefjord, K., Söderberg, R., Lindkvist, L.. Individualizing locator adjustments of assembly fixtures using a digital twin. J Comput Inf Sci Eng 2019;19(4):041019. doi:https://doi.org/10.1115/1.4043529.

[15] Tabar, R.S., Söderberg, R., Ceglarek, D., Franciosa, P., Lindkvist, L.. Augmented geometry assurance digital twin with physics-based incremental learning. CIRP Ann 2025;doi:https://doi.org/10.1016/j.cirp.2025.03.008.

[16] Nocedal, J., Wright, S.J.. Numerical optimization. Springer, New York, NY; 2006. doi:https://doi.org/10.1007/978-0-387-40065-5.

[17] Lindkvist, L., Carlson, J.S., Söderberg, R.. Virtual locator trimming in pre-production: rigid and non-rigid analysis. In: ASME Int. Mech. Eng. Congr. Expo.; vol. 42231. 2005, p. 561–568. doi:https://doi.org/10.1115/IMECE2005-81266.

[18] Soden, P.D., Hinton, M.J., Kaddour, A.. Lamina properties, lay-up configurations and loading conditions for a range of fibre reinforced composite laminates. In: Failure criteria in fibre-reinforced-polymer composites. Elsevier; 2004, p. 30–51. doi:https://doi.org/10.1016/B978-008044475-8/50003-2.

[19] Söderberg, R., Wärmefjord, K., Lindkvist, L.. Variation simulation of stress during assembly of composite parts. CIRP Annals 2015;64(1):17–20. doi:https://doi.org/10.1016/j.cirp.2015.04.048.